Pigment Organization and Energy Transfer Dynamics in Isolated Photosystem I (PSI) Complexes from *Arabidopsis thaliana* Depleted of the PSI-G, PSI-K, PSI-L, or PSI-N Subunit

Janne A. Ihalainen,* Poul Erik Jensen,† Anna Haldrup,† Ivo H. M. van Stokkum,‡ Rienk van Grondelle,‡ Henrik Vibe Scheller,† and Jan P. Dekker‡

*Department of Chemistry, University of Jyväskylä, FIN-40351 Jyväskylä, Finland; †The Royal Veterinary and Agricultural University, DK-1871 Copenhagen, Denmark; and ‡Faculty of Sciences, Division of Physics and Astronomy, Vrije Universiteit, 1081 HV Amsterdam, The Netherlands

ABSTRACT Green plant photosystem I (PSI) consists of at least 18 different protein subunits. The roles of some of these protein subunits are not well known, in particular those that do not occur in the well characterized PSI complexes from cyanobacteria. We investigated the spectroscopic properties and excited-state dynamics of isolated PSI-200 particles from wild-type and mutant *Arabidopsis thaliana* plants devoid of the PSI-G, PSI-K, PSI-L, or PSI-N subunit. Pigment analysis and a comparison of the 5 K absorption spectra of the various particles suggests that the PSI-L and PSI-H subunits together bind approximately five chlorophyll *a* molecules with absorption maxima near 688 and 667 nm, that the PSI-G subunit binds approximately two red-shifted β-carotene molecules, that PSI-200 particles without PSI-K lack a part of the peripheral antenna, and that the PSI-N subunit does not bind pigments. Measurements of fluorescence decay kinetics at room temperature with picosecond time resolution revealed lifetimes of ~0.6, 5, 15, 50, 120, and 5000 ps in all particles. The 5- and 15-ps phases could, at least in part, be attributed to the excitation equilibration between bulk and red chlorophyll forms, though the 15-ps phase also contains a contribution from trapping by charge separation. The 50- and 120-ps phases predominantly reflect trapping by charge separation. We suggest that contributions from the core antenna dominate the 15-ps trapping phase, that those from the peripheral antenna proteins Lhca2 and Lhca3 dominate the 50-ps phase, and that those from Lhca1 and Lhca4 dominate the 120-ps phase. In the PSI-200 particles without PSI-K or PSI-G protein, more excitations are trapped in the 15-ps phase and less in 50- and 120-ps phases, which is in agreement with the notion that these subunits are involved in the interaction between the core and peripheral antenna proteins.

INTRODUCTION

Green plant photosystem I (PSI) is one of the four major complexes responsible for the light reactions in oxygenic photosynthesis. It is bound to the thylakoid membranes of chloroplasts, uses light to catalyze the oxidation of plastocyanin and the reduction of $NADP^+$, and also contributes to the transmembrane pH gradient. The complex consists of at least 18 different types of protein subunits, 14 of which form the so-called core complex (Chitnis, 2001; Scheller et al., 2001). The core complex binds ~100 chlorophyll *a* (Chl *a*) molecules and is responsible for all electron transfer reactions between plastocyanin and $NADP^+$. The subunits of the PSI core complex are denoted PSI-A to PSI-O, most of which are conserved among all organisms performing oxygenic photosynthesis. Exceptions are the PSI-G, -H, -N, and -O subunits, which are found only in eukaryotic photosynthetic organisms (Scheller et al., 2001; Knoetzel et al., 2002). These organisms also contain a peripheral antenna complex known as light-harvesting complex I (LHCI), which consists of four types of proteins (called Lhca1–4). Approximately two copies of each of these proteins bind to the PSI core complex, and together these proteins bind another 80–100 Chl ($a + b$) molecules. These proteins belong to the group of proteins encoded by the Lhc supergene family and have protein masses in the range of 20–24 kDa (Jansson, 1994).

The structure of the PSI core complex from the cyanobacterium *Synechococcus elongatus* has been resolved at 2.5 Å resolution (Jordan et al., 2001; Fromme et al., 2001). A high-resolution structure is not available for PSI from higher plants. A low-resolution study by electron microscopy and single-particle image analysis revealed that the LHCI proteins are bound only on the side of the PSI core complex occupied by the PSI-F and PSI-J subunits (Boekema et al., 2001a). A similar location was recently found for a peripheral antenna complex of PSI from cyanobacteria grown under iron stress (Bibby et al., 2001; Boekema et al., 2001b).

The main building block of the PSI core complex is formed by the large PSI-A and PSI-B subunits, which bind most of the core antenna pigments and also the photochemical reaction center (Jordan et al., 2001). However, also the small subunits, some of which are the subject of this paper, have important functions in the photosynthetic performance of green plant PSI (Scheller et al., 2001). PSI-K, for instance, is a small protein with two transmembrane α-helices, which in cyanobacteria is located at the periphery of the

Submitted March 27, 2002, and accepted for publication May 29, 2002.

Address reprint requests to Dr. Jan P. Dekker, Faculty of Sciences, Division of Physics and Astronomy, Vrije Universiteit, De Boelelaan 1081, 1081 HV Amsterdam, The Netherlands. Tel.: 31-20-4447931; Fax: 31-20-4447999; E- mail: dekker@nat.vu.nl.

0006-3495/02/10/2190/12 $2.00

complex (Jordan et al., 2001). Green plants have a similar protein (Kjaerulff et al., 1993), and it has been observed that PSI-200 particles devoid of the PSI-K subunit have lost ~20–30% of the Lhca2 protein and ~30–40% of the Lhca3 protein (Jensen et al., 2000). PSI-K may therefore be involved in the binding of LHCI to the PSI core. PSI-G is structurally related to PSI-K, but unlike PSI-K it does not occur in cyanobacteria. Moreover, PSI-200 particles without PSI-G have a normal content of all LHCI proteins, though under mildly denaturing conditions a more unstable interaction between the PSI core and the LHCI antenna was observed (Jensen et al., 2002). Interestingly, deletion of PSI-G resulted in a significantly increased $NADP^+$ reduction rate, and it was suggested that PSI-G is involved in the regulation of the electron transport efficiency of PSI (Jensen et al., 2002).

In cyanobacteria, PSI-L has been shown to be required for the assembly of PSI trimers (Chitnis and Chitnis, 1993), a process that probably requires the binding of calcium ions to the PSI-L subunit (Schwabe et al., 2001). In some cyanobacteria, the trimerization causes an enhancement of red absorption of PSI complex (see below). Green plants also contain PSI-L, but trimeric PSI particles have never been found in these organisms. *Arabidopsis thaliana* plants with down-regulated PSI-L synthesis also show a secondary loss of PSI-H, suggesting an interaction between PSI-H and PSI-L (Scheller et al., 2001). PSI-H has been shown to be involved in the so-called state transitions (Lunde et al., 2000; Haldrup et al., 2001), which suggests that PSI-H may form a binding site for trimeric LHCII. But overall, the role of PSI-L is not yet known. PSI-N is found only in PSI from higher plants. It is an extrinsic protein located at the lumen side of the membrane and has been shown to have interaction with PSI-F. Both proteins have been shown to be involved in the docking of plastocyanin and therefore influence the reduction quality of PSI in higher plants (Haldrup et al., 1999, 2000).

A general feature of PSI in almost all organisms is the presence of chlorophylls with energy levels lower than that of reaction center chlorophyll P700. In green plant PSI, several of such red pigments have been observed. The red-most pigments are located in LHCI and show at cryogenic temperatures broad absorption and emission bands with maxima at ~715 and 735 nm, respectively (see, e.g., Croce et al., 1998; Ihalainen et al., 2000; Ganeteg et al., 2001). The core complex binds red pigments with a low temperature emission maximum at around 720 nm (Croce et al., 1998). In cyanobacterial PSI, the energy and amount of red chlorophylls is variable (see, e.g., Gobets and van Grondelle, 2001) and depends on the species and growth conditions.

The excitation energy transfer rates between the antenna pigments and pigment pools can be studied by means of time-resolved fluorescence or absorption spectroscopy (see for review van Grondelle et al., 1994). The single-step energy transfer times between chlorophylls in the PSI antenna have been measured to be ~100–200 fs (Du et al., 1993; Kennis et al., 2001), in agreement with simulations based on the Förster energy transfer model (Gobets and van Grondelle, 2001; Beddard, 1998). The equilibration of the excitation energy among the bulk antenna chlorophylls in the PSI core complex takes place in ~500 fs, whereas the equilibration with the red chlorophylls is between 2 and 15 ps in the various systems, including the green plant PSI-200 (Gobets and van Grondelle, 2001). The overall trapping of the excitation energy occurs in PSI core complexes in 20–50 ps, depending on the amount and energies of the red chlorophylls (Gobets and van Grondelle, 2001), whereas in the green plant PSI-200 complex biphasic trapping kinetics of ~60 and 130 ps have been reported (Croce et al., 2000).

In this paper we present a detailed characterization of the spectroscopy and excitation dynamics of isolated PSI-200 particles obtained from wild-type *Arabidopsis thaliana* plants and of its mutants lacking the PSI-G, PSI-K, PSI-L, or PSI-N subunits. Comparison of 5 K absorption spectra of the various particles suggests that the PSI-L and PSI-H subunits bind chlorophylls, peaking at 688 and 667 nm, and that the PSI-G subunit binds one or two red-shifted β-carotene molecules. Comparison of the fluorescence dynamics of the various particles indicates that without the PSI-K or PSI-G subunits the relative trapping proportions by the core and peripheral antenna systems are increased and decreased, respectively. Some of the results have been presented at the 12th International Congress on Photosynthesis (Ihalainen et al., 2001).

MATERIALS AND METHODS

PSI-200 particles were prepared from wild-type *Arabidopsis thaliana* and lines lacking the PSI-G, PSI-K, PSI-L, or PSI-N subunits by *n*-dodecyl-β,D-maltoside (β-DM) solubilization and sucrose density gradient centrifugation as described by Jensen et al. (2000). For pigment analysis the PSI-200 particles were extracted with 80% acetone under dim, green light. The pigment composition was analyzed with a Dionex HPLC system with a Waters Spherisorb analytical column, ODS1 (250- × 4.6-mm internal dimensions; 5-μm particle size). The mobile phase consisted of two solvents: A, with acetonitrile/methanol/water (84:9:7), and B, with methanol/ethylacetate (68:32), both containing 0.1% triethylamine. The pigments were eluted with a linear gradient from 100% A to 100% B over 10 min, followed by an isocratic elution with 100% B for 5 min, and a linear gradient of 100% B to 100% A in 1 min. The column was regenerated with 100% solvent A for 20 min before injection of the next sample. Injection volume was 80 μl, the flow rate was 1 ml min^{-1}, and the eluate was monitored with a photodiode array detector in the range of 290–595 nm. Pigments were identified by comparing retention times and absorption spectra with standard pigments (DHI, Horsholm, Denmark). Quantification was performed by integration of the elution peaks at 445 nm using the program Chromeleon version 6 (Dionex, Sunnyvale, CA).

For the spectroscopic measurements, the isolated complexes were diluted in 20 mM Bis-Tris (pH 6.5), 20 mM NaCl, and 0.06% β-DM to an optical density of 0.6 cm^{-1} at 680 nm. For the time-resolved fluorescence measurements, 10 mM sodium ascorbate and 10 μM phenazine metasulfate were added, whereas for the low-temperature measurements 66% (v/v)

glycerol was added as cryoprotectant. Fluorescence emission spectroscopy was performed with equipment described by Ihalainen et al. (2000).

The time-resolved measurements were performed with a streak camera described in detail by Gobets et al. (2001b). In short, excitation pulses of 475 or 710 nm (~100 fs) were generated using a titanium:sapphire laser (MIRA, Coherent, St. Clara, CA) with regenerative amplifier (Coherent, REGA) and a double-pass optical parametric amplifier (Coherent, OPA). The repetition rate was 150 kHz, and the pulse energy was below 1 nJ for 475-nm excitation and ~3 nJ for 710-nm excitation. The excitation light was collimated with a 15-cm focal length lens, resulting in a focal diameter of 150 μm in the sample. The sample was placed into a 2-mm-thick spinning cell with rotation speed of 30 Hz. The fluorescence was detected through colored glass filters and/or polarizers at right angles with respect to the excitation beam, using a Hamamatsu C5680 synchroscan streak camera and a Chromex 250IS spectrograph. The polarization of the fluorescence light was at magic angle (475-nm excitation) or perpendicular to the polarization of the excitation light (710-nm excitation). The streak images were recorded with a cooled Hamamatsu C4880 CCD camera. The exposure times were 10 and 15 min for 200- and 800-ps time bases, respectively. The images were integrated together and analyzed by using a unidirectional sequential model with increasing lifetimes, which produces the so-called species-associated spectra (SAS). With 475-nm excitation, the first SAS (representing the time 0 spectrum) was constrained to be zero in the Q_y region. From the SAS, the decay-associated spectra (DAS) were determined, which are linear combinations of the SAS (Holzwarth, 1996). These DAS are the amplitudes of the exponential fluorescence decay components (Holzwarth, 1996). The instrument response function was modeled as a Gaussian with FWHM of 3.9 and 10 ps for the 200- and 800-ps time bases, respectively. All emission spectra were corrected for the spectral sensitivity of the apparatus.

RESULTS

Biochemical characterization

Arabidopsis thaliana lines lacking the PSI-G, -K, -L, or -N subunits of PSI have previously been prepared and biochemically characterized (Haldrup et al., 1999; Jensen et al., 2000, 2002; Lunde et al., 2000), and PSI-200 complexes could be isolated and purified with comparable yields from the wild-type plants and all mutants. In some of the lines and PSI-200 complexes, analysis of the subunit composition using SDS-polyacrylamide gel electrophoresis and immunoblotting revealed secondary loss of other PSI subunits. In the absence of PSI-K, a 30–40% reduction of Lhca2 and Lhca3 was seen (Jensen et al., 2000), whereas in the absence of PSI-L a 90% reduction in PSI-H was observed (Lunde et al., 2000). In the absence of PSI-N no significant loss of other subunits from the purified PSI-200 complexes was detected (Haldrup et al., 1999). In the lines lacking PSI-G there was also no loss of other subunits, but in some lines a residual amount of PSI-G was still present, both in the cells and in the PSI-200 particles (Jensen et al., 2002). In the particles investigated in this study, the residual amount of PSI-G was 8% or less. The secondary losses of other subunits are summarized in Table 1.

The pigment composition of the investigated particles is shown in Table 2. The chlorophyll and carotenoid contents of all particles do not differ very much, which is consistent with the notion that they all contain the major pigment-binding proteins (the PSI-A and PSI-B subunits of the core complex and the LHCI proteins). However, in the absence of PSI-K, the contents of Chl *b* and lutein are slightly lower, as expected from the partial absence of Lhca2 and Lhca3 (Jensen et al., 2000), whereas in the absence of PSI-G the β-carotene content is somewhat lower. All other differences are within the error margins of the pigment determinations.

TABLE 1 Secondary loss of protein subunits in PSI-200 complexes purified from plant lines with primary loss of PSI-G, PSI-K, PSI-L, or PSI-N

Plant line	Primary loss	Secondary loss (%)	Reference
ΔPSI-G	PSI-G	None	Jensen et al. (2002)
ΔPSI-K	PSI-K	~30% Lhca2 ~40% Lhca3	Jensen et al. (2000)
ΔPSI-L	PSI-L	~90% PSI-H	Lunde et al. (2000)
ΔPSI-N	PSI-N	None	Haldrup et al. (1999)

Absorption spectra at 5 K

Fig. 1 shows 5 K absorption spectra of PSI-200 particles from wild-type *Arabidopsis* and the studied mutants. The spectra were normalized to the area of the Chl Q_y-absorption band. All spectra are similar, which is not surprising, because the PSI-K and PSI-L subunits of *S. elongatus* bind only a few pigments (Jordan et al., 2001) and because the PSI-G and PSI-N subunits are not expected to bind many pigments either.

More information about the various absorption spectra can be obtained by analyzing the 5 K absorption difference spectra of the various PSI-200 particles. A problem with this approach is the normalization of the spectra, which is arbitrary because there is no reliable way to estimate the concentration of PSI with a precision of 99% or better. Such a precision is required if a difference caused by the absence of a single pigment is to be recorded. The normalization problem was also noted by Soukoulis et al. (1999), who used a similar approach to estimate the influence of the absence of small subunits in PSI from *Synechocystis* sp. PCC 6803. Based on difference spectra of PSI-200 particles obtained

TABLE 2 Pigment composition of the PSI-200 complexes from wild-type *Arabidopsis* and lines without PSI-G, PSI-K, PSI-L, or PSI-N

Pigment	Wild type	ΔPSI-G	ΔPSI-K	ΔPSI-L	ΔPSI-N
Violaxanthin	3.0 ± 0.3	3.1 ± 0.4	2.9 ± 0.3	2.6 ± 0.3	3.3 ± 0.3
Lutein	5.6 ± 0.8	5.5 ± 0.9	4.8 ± 0.7	5.8 ± 1.4	5.5 ± 0.3
β-Carotene	15.4 ± 0.5	13.7 ± 1.4	15.6 ± 0.7	15.3 ± 0.3	14.8 ± 0.5
Chl *a*	100	100	100	100	100
Chl *b*	10.1 ± 1.9	9.9 ± 1.6	9.2 ± 0.9	10.3 ± 1.5	10.3 ± 4.2
Chl *a*/*b*	9.9 ± 1.8	10.1 ± 1.6	10.9 ± 1.0	9.7 ± 1.4	9.7 ± 4.3

Pigment composition was determined by HPLC. Shown are the averages ± SD of two to three independent determinations. The pigment contents are expressed per 100 Chl *a* molecules.

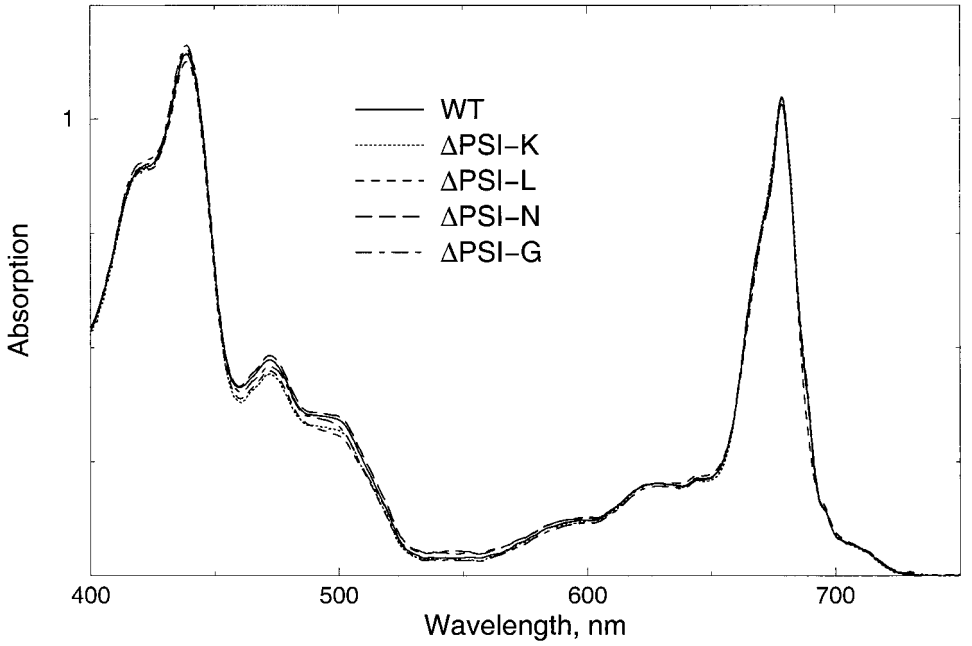

FIGURE 1 The 5 K absorption spectra of isolated PSI-200 complexes from wild-type *Arabidopsis thaliana* and its mutants lacking PSI-K, PSI-L, PSI-N, or PSI-G subunit. The spectra were normalized to the area of the Q_y-absorption region and to an absorption of 1.0 at 680 nm for the wild-type spectrum.

from different lines of wild-type *Arabidopsis* we estimate that the accuracy of these measurements is ~0.02 OD units around the absorption maximum at 679 nm (if $OD_{679} = 1$) and that the accuracy is better in regions of lower absorption.

The largest difference between the 5 K absorption spectra of PSI-200 particles from wild-type and mutant *Arabidopsis* lines was observed between those of the PSI-L mutant and the wild-type. Even in the spectra shown in Fig. 1 it is obvious that the spectrum of the PSI-L mutant (short dashes) deviates from the other spectra in several wavelength regions. To get a better idea of the differences in the absorption spectra, we present in Fig. 2 *A* a difference spectrum constructed by assuming that the PSI-L and PSI-H subunits together bind five Chl *a* molecules. This assumption was based on the finding that the PSI-L subunit in *S. elongatus* binds three Chl *a* molecules (Jordan et al., 2001) and on the idea that the PSI-H subunit binds a few chlorophylls as well. If PSI-H binds LHCII in state 2, as may be concluded from its involvement in the state transitions (Lunde et al., 2000), then energy transfer from LHCII to PSI will probably be facilitated if PSI-H binds chlorophyll. The difference spectrum in Fig. 2 *A* shows clear minima at 688 and 667 nm with significant amplitude. The same conclusion could be drawn if slightly different normalizations were chosen (not shown). These results suggest that PSI-L and PSI-H of *Arabidopsis* indeed bind Chl *a* and that these molecules absorb maximally at 688 and 667 nm. We note that the absence of PSI-L in *Synechocystis* sp. PCC 6803 resulted in a main difference at 700 nm (Soukoulis et al., 1999), but this difference could also originate from the absence of monomer-monomer interactions in the PSI-L mutant, as noted by the authors. Our *Arabidopsis* complexes, however, were all in the monomeric aggregation state, and monomer-monomer interactions do not play a role in our difference spectra. The difference spectrum of Fig. 2 *A* also shows a minimum at 499 nm, which suggests that PSI-L and/or PSI-H bind β-carotene molecules peaking at 499 nm. In PSI from *S. elongatus* it has been shown that some of the β-carotene molecules indeed have contacts with the PSI-L subunit (Jordan et al., 2001). We note that 77 K linear dichroism and circular dichroism spectra did not reveal significant differences between the PSI-L mutant and the wild type (Ihalainen et al., 2001), which suggests that the 688- and 667-nm chlorophylls do not contribute very significantly to these spectra.

The difference spectra of the PSI-K mutant minus the wild type also revealed some differences (not shown), but these are clearly dominated by the partial absence of Lhca2 and Lhca3 (Jensen et al., 2000), which mask the changes caused by the possible absence of chlorophylls and/or carotenoids bound to PSI-K. The PSI-K subunit binds two Chl *a* molecules in *S. elongatus*. However, the absence of PSI-K in *Synechocystis* PCC 6803 did not cause very significant absorption changes (Soukoulis et al., 1999).

A difference spectrum of the PSI-G mutant and the wild type is presented in Fig. 2 *B*. This spectrum was prepared on the basis of equal oscillator strengths in the $Q_{y(0-0)}$ absorp-

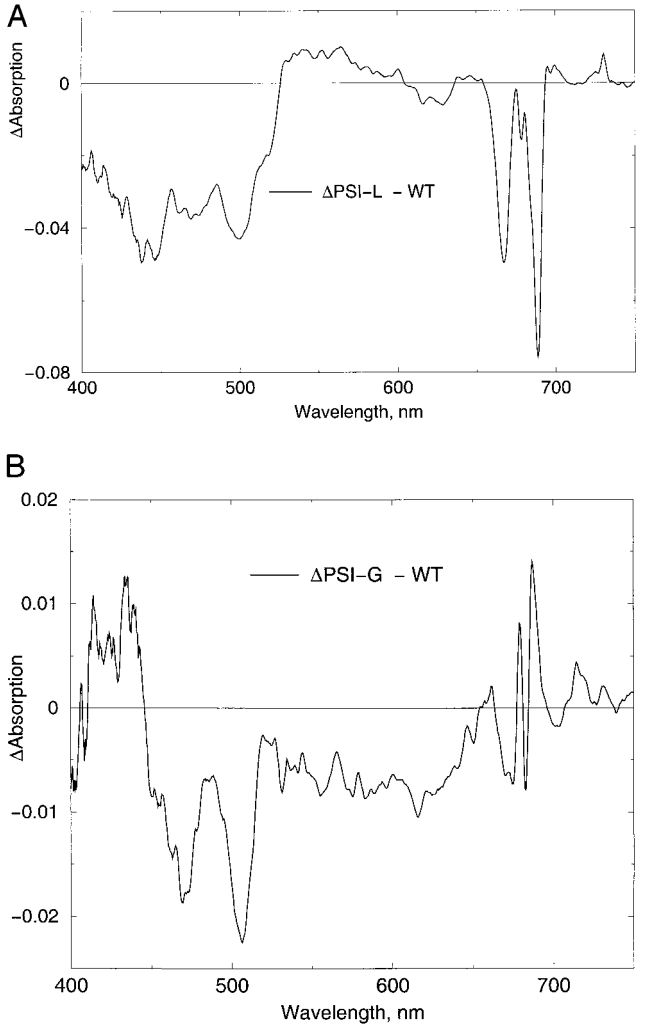

FIGURE 2 The 5 K absorbance difference spectra between PSI-200 particles from the wild-type and the PSI-L-deficient (*A*) and PSI-G-deficient (*B*) plants. The spectra were normalized on the basis of the presence of five (*A*) and no (*B*) chlorophylls in the missing subunits in the mutants.

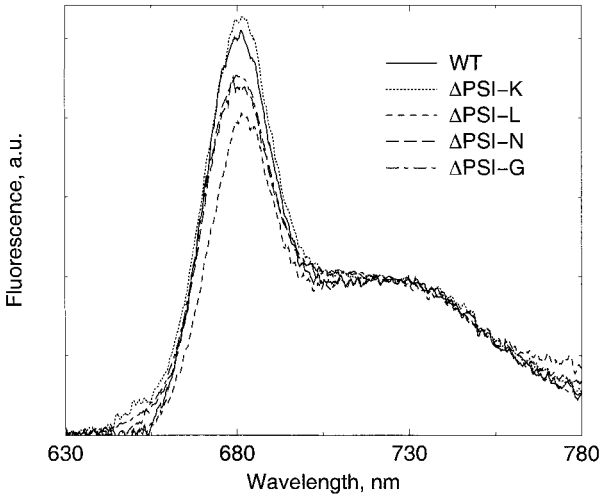

FIGURE 3 Room-temperature emission spectra of isolated PSI-200 particles of wild-type *Arabidopsis* (——) and its mutants missing the PSI-K (· · ·), PSI-L (– – –), PSI-N (— — —), and PSI-G (· — ·) subunits after 435-nm continuous light excitation. The spectra were normalized to the red wing of the spectra.

tion regions of Chl *a* in both spectra. There is no obvious justification for the assumption of no Chl *a* binding to PSI-G, other than the very similar Chl *a*/*b* ratios in the wild type and PSI-200 particles without PSI-G (see Table 2) and because the PSI-G protein does not occur in the 2.5-Å structure of PSI from *S. elongatus*. The difference spectrum in Fig. 2 *B*, however, shows, apart from some rather small and probably insignificant changes around 680 nm, pronounced bands at 506 and 469 nm to be missing in the absence of PSI-G. Normalizations based on the presence of one or two Chl *a* molecules in PSI-G revealed similar differences in the carotenoid absorption region (not shown). It is very likely that the missing carotenoid is β-carotene, because β-carotene is the only carotenoid in the PSI core complex and because the pigment quantitation indicates that the PSI-G mutant has a lower β-carotene content (Table 2). The amplitude of the difference spectrum is compatible with a difference of one to two carotenoids, whereas the pigment quantitation suggests a difference of two to three β-carotenes (assuming the presence of 160–170 Chl *a* molecules in one PSI-200 particle). The β-carotenes of PSI-G absorb more to the red than most β-carotenes in higher plant PSI, because the low-temperature absorption spectrum of the isolated PSI core complex from higher plants shows maxima at 502 and 466 nm (J. A. Ihalainen and B. Gobets, unpublished results).

The difference spectrum of the PSI-N mutant and the wild type revealed only some minor and insignificant deviations in the Chl *a* Q_y absorption region ($\Delta OD < 0.02$, not shown). This suggests that PSI-N, the only extrinsic subunit of PSI located at the lumen side of the membrane, does not bind pigments, just like the extrinsic subunits at the stroma side of the membrane (Scheller et al., 2001) and that the absence of PSI-N has only minor effects on the entire pigment network.

Steady-state emission at room temperature

Room-temperature steady-state emission spectra of the PSI-200 complexes from the wild-type and mutant *Arabidopsis* lines are shown in Fig. 3. All spectra consist of a pronounced peak at ~680 nm and a broad feature near 730 nm. The spectra were recorded in the presence of 0.06% β-DM, which is clearly above the critical micelle concentration (~0.009% for β-DM). Under these conditions, the room-temperature emission spectra of PSI-200 and PSI core complexes usually reveal a band around 680 nm, which originates from a few Chl *a* molecules that cannot efficiently

deliver their excitation energy to the reaction center chlorophyll P700 (Croce et al., 1996; Pålsson et al., 1998). These chlorophylls have probably very long lifetimes (see also below) and therefore give a very significant contribution to the steady-state emission spectrum. It was shown by Croce et al. (1996) that lowering the detergent concentration to below the critical micelle concentration strongly diminished the 680-nm contribution. For the experiments described here, however, we did not lower the detergent concentration, because in that case significant particle aggregation is expected, which could introduce new energy transfer pathways between monomers. The band around 730 nm originates from the red chlorophylls of PSI-200 (F-730 and F-720, which belong to LHCI and the PSI core complex, respectively).

As in the case of the 5 K absorption spectra, the main features of the emission spectra of all investigated PSI particles are quite similar. The most pronounced difference was again observed for the PSI-L mutant, which shows a smaller and slightly red-shifted (to 682 nm) uncoupled Chl contribution (Fig. 3). It is tempting to speculate that some of the chlorophylls of the PSI-L and/or PSI-H subunits contribute to the 680-nm emission, in particular those absorbing at 667 nm at 5 K. The chlorophylls of PSI-L of *S. elongatus* are in fact located in the periphery of the monomeric complex (Jordan et al., 2001) and may therefore have some direct contacts with the detergent.

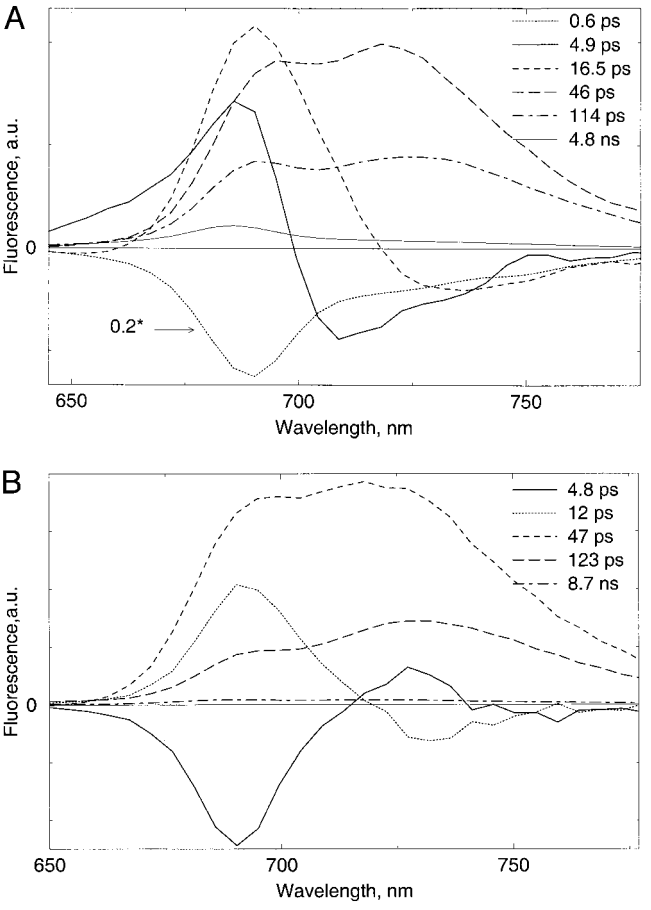

FIGURE 4 DAS of fluorescence decay of isolated PSI-200 complexes from wild-type *Arabidopsis thaliana* at room temperature after 475-nm (*A*) and 710-nm (*B*) excitation. For both excitation wavelengths, ~65% of the excitation energy was absorbed by LHCI and ~35% by the PSI core complex.

Time-resolved fluorescence of PSI-200 from wild-type *Arabidopsis*

We investigated the fluorescence decay kinetics at room temperature of the various PSI-200 particles by a setup consisting of a synchroscan streak camera in combination with a spectrograph, which has an instrumental response of ~3 ps and which enables us to observe kinetics occurring slightly faster than 1 ps. This technique has recently been applied to PSI core complexes from various cyanobacteria (Gobets et al., 2001b) and to a mixture of dimeric LHCI complexes from maize (Gobets et al., 2001a). The instrumental response of the streak-camera technique is approximately an order of magnitude better than that of the more commonly applied single-photon timing technique. With the latter technique, the fluorescence decay kinetics of PSI-200 complexes from maize has recently been analyzed (Croce et al., 2000).

Fig. 4 shows DAS resulting from the global analysis of the fluorescence kinetics of PSI-200 from wild-type *Arabidopsis* after 475 nm (Fig. 4 *A*) and 710 nm (Fig. 4 *B*) excitation. The 475-nm pulses excited mainly carotenoid and Chl *b* molecules, whereas the 710-nm pulses mainly excited the red pigments of PSI-200. In both cases, ~65% of the excitations are expected to be absorbed by LHCI and ~35% by the PSI core. These estimates are based on a comparison of the room-temperature absorption spectra of isolated PSI core and LHCI antenna complexes.

The data detected after 475-nm excitation could be fitted satisfactorily with six components (Fig. 4 *A*). The fastest component has a lifetime of 0.6 ps and exhibits a strong negative band in the Chl *a* Q_y absorption region. A very similar component has been observed upon 470-nm excitation of LHCI (Gobets et al., 2001a), which was ascribed to relaxation from higher Chl states to the Q_y state and to energy transfer from carotenoids to Chl *a* molecules. Fluorescence up-conversion studies have revealed that a large part of the energy transfer from carotenoids to chlorophylls is extremely fast (within 0.2 ps), both in PSI core complexes (Kennis et al., 2001) and in LHCI (Gobets et al., 2001a), and therefore should contribute significantly to the fastest component.

The 4.9- and 16.5-ps components are characterized by positive features around 680 nm and negative features above 695 and 720 nm, respectively. Both can be attributed,

at least in part, to the excitation equilibration between bulk and red chlorophyll forms (4.9 ps), followed by an additional equilibration with far-red chlorophylls forms (16.5 ps). A 4–5-ps phase with a similar spectrum has also been observed in several cyanobacterial core complexes upon 400-nm excitation (Gobets et al., 2001b) and 505-nm excitation (B. Gobets, unpublished observations) and in LHCI upon 470-nm excitation (Gobets et al., 2001a), which suggests that this phase originates from energy transfer processes both in the PSI core and LHCI antenna systems. A 2–3-ps process has also been observed (with pump-probe absorbance-difference spectroscopy) in PSI core complexes from *Chlamydomonas reinhardtii*, but these particles probably lack red pigments (Gibasiewicz et al., 2001). The 16.5-ps component is nonconservative (the positive contributions are much stronger than the negative) and similar in shape to the 10-ps component observed in the PSI core complex of *S. elongatus*. The latter component was interpreted as a combination of bulk/C708 equilibration with far-red pigments (C719) and trapping by charge separation (Gobets et al., 2001b, and unpublished results). A component with similar time constant and spectral characteristics has also been observed in isolated LHCI (Gobets et al., 2001a). In these particles, the 10-ps component was ascribed to intermonomer energy transfer (Melkozernov et al., 1998; Gobets et al., 2001a), whereas the nonconservative character was explained by a lowered oscillator strength of the red state (Gobets et al., 2001a). We note that with the single-photon timing technique a single component of 11 ps was observed in PSI-200 (Croce et al., 2000), which most likely is a mixture of both the 4.9- and 16.5-ps components resolved by the streak-camera technique.

The components of 46 and 114 ps have all-positive spectra and correspond to the time of the trapping of the excitation energy by charge separation in the reaction center. Similar kinetics has been reported for PSI-200 from maize (Croce et al., 2000) and spinach (Turconi et al., 1994). The most straightforward explanation of the two lifetimes is that the first trapping phase mainly involves photons in the PSI core antenna and that the second trapping phase mainly involves photons in LHCI, in agreement with the peak maxima of both components (Fig. 4 *A*). The 46-ps phase peaks near 720 nm, close to the emission maximum of the long-wavelength chlorophylls of the core antenna complex, whereas the 114-ps phase peaks above 725 nm, which can be explained by a relatively larger contribution from the peripheral antenna. An alternative explanation would be that the 46-ps phase has more contributions from the Lhca2 and Lhca3 complexes and that the 114-ps phase has more contributions from the Lhca1 and Lhca4 proteins, because the emission of Lhca2 and/or Lhca3 is blue-shifted compared with that of Lhca1 and Lhca4 (Ihalainen et al., 2000; Ganeteg et al., 2001). We note that our spectra and those of Turconi et al. (1994) were recorded in the presence of detergent, and both include a contribution at 680 nm in the two components, whereas those of Croce et al. (2000), recorded in the absence of detergent, lack the 680-nm feature. Our data reveal that the 680-nm feature in the slowest trapping component is also much less pronounced after 710-nm excitation (shown and discussed below).

The last component has a long lifetime of ~4.8 ns but a very low amplitude (Fig. 4 *A*) and originates from chlorophylls that are unable to transfer their excitation energy to the reaction center. It probably arises from some uncoupled or free LHCI complexes and some uncoupled Chl *a* and Chl *b* molecules, although the absorption of Chl *a* is really low at 475 nm.

For the 710-nm dataset, the fluorescence was recorded perpendicularly to the polarization of the excitation light to avoid scattering artifacts as much as possible. Five components were needed to describe the data. All lifetimes were similar to the five slowest lifetimes needed to describe the dataset obtained with 475-nm excitation. The first phase occurs with a lifetime of 4.8 ps (Fig. 4 *B*) and clearly reflects the equilibration of the excitation energy among the red chlorophylls and the bulk antenna pigments. The fact that the negative amplitude around 690 nm (reflecting the ingrowth of the fluorescence at shorter wavelengths) is larger than the decay around 720 nm is probably related to the perpendicular polarization of the excitation light. It is furthermore remarkable that the DAS of the slowest trapping component (the 123-ps phase) shows a considerably smaller 680-nm feature than after 475-nm excitation (Fig. 4 *A*). This suggests that some of the free chlorophylls, which are more easily excited by 475-nm light than by 710-nm light, decay within the 123-ps phase and thus do not formally belong to the free, or unconnected, chlorophylls. The long-living component has a spectrum that resembles that of isolated LHCI (Gobets et al., 2001a) and can be assigned to partially uncoupled or unfavorably oriented LHCI complexes. This component is probably also present after 475-nm excitation, but in this case the slow kinetics are dominated by free Chl *a* and Chl *b* molecules, which do not absorb at all at 710 nm. We note that the lifetime of the long-lived component is much longer than the applied maximal time base (800 ps) and must be regarded as a very crude approximation. The analysis of isolated LHCI also revealed a minor 0.6-ns long-lived component (Gobets et al., 2001a), but this component could not be resolved in our analysis of the PSI-200 fluorescence kinetics, because of the small amplitude of the long-lived components in PSI-200.

Time-resolved fluorescence of PSI-200 from *Arabidopsis* mutants

We also recorded the fluorescence kinetics of the PSI-200 particles from the *Arabidopsis* plants without PSI-G upon 710-nm excitation and of the PSI-200 particles from the *Arabidopsis* plants without PSI-K, PSI-L, and PSI-N upon both 475- and 710-nm excitation. After a first inspection of

the data it became immediately clear that the differences between the various datasets were very small (not shown). This was actually expected, because in most particles the general organization of the peripheral and core antenna chlorophylls probably does not differ very significantly and because there are no mutant-induced changes expected for the charge separation efficiency of P700.

To highlight possible differences in the fluorescence kinetics between the PSI-200 particles from the various mutants, we analyzed the data under the constraint of identical kinetics in all investigated particles and looked for differences in the yields and spectra of the various components. This type of approach is probably justified as a first approximation, because fitting with completely free parameters did not result in significantly better residuals in any of the datasets. The results of this approach are shown in Fig. 5 for the 475-nm excitation and Fig. 6 for the 710-nm excitation and reveal no significant differences between the wild-type and the PSI-L mutant (Figs. 5 *b* and *c*) and between the wild-type and the PSI-N mutant (Figs. 5 *c* and *d*). However, in the PSI-K (Figs. 5 *a* and *b*) and PSI-G mutants (Fig. 6 *a*), the spectrum of the second energy transfer phase of 12–16.5 ps is more nonconservative than in the wild type and in the other mutants. This means that in the PSI-200 particles without the PSI-K or PSI-G subunits a larger part of the excitation energy is trapped within the 12–16.5-ps phase than in the other particles. This also means that the trapping in this phase is dominated by trapping by charge separation in the reaction center and not by trapping in LHCI, because the PSI-K mutants have a smaller LHCI antenna.

In Tables 3 and 4 we plot the proportions of the various trapping components. These proportions were calculated from the integrated areas of the components from the global analysis of the datasets obtained with 475-nm excitation (Table 3) and 710-nm excitation (Table 4). The results in Tables 3 and 4 show that in particular the trapping efficiency of the 47-ps phase has decreased in the PSI-K and PSI-G mutants. In the case of the PSI-K mutant, a decrease of the 47-ps phase can be understood if this phase contains dominant contributions from the Lhca2 and Lhca3 proteins (see above), because this mutant lacks ~30% of these proteins (Jensen et al., 2000). In the case of the PSI-G mutant, the increased 12-ps trapping and decreased 47-ps trapping could be interpreted as an increased trapping efficiency in the core antenna and a decreased energy transfer from the core antenna to Lhca2 and Lhca3, in agreement with the results of Jensen et al. (2002).

The DAS of the 8.7-ns phase of the various particles upon 710-nm excitation are shown in Fig. 7. These spectra mainly reflect the contributions from unconnected or badly connected LHCI antenna complexes and contain almost no contributions from free chlorophylls observed upon 475-nm excitation (see above). The data suggest that the PSI-200 particles from PSI-G mutant contain the largest amount of badly connected LHCI, whereas those from the PSI-L mutant show the smallest amount. Also after 475-nm excitation, the PSI-L mutant revealed the smallest contribution from unconnected chlorophylls (not shown). The DAS from

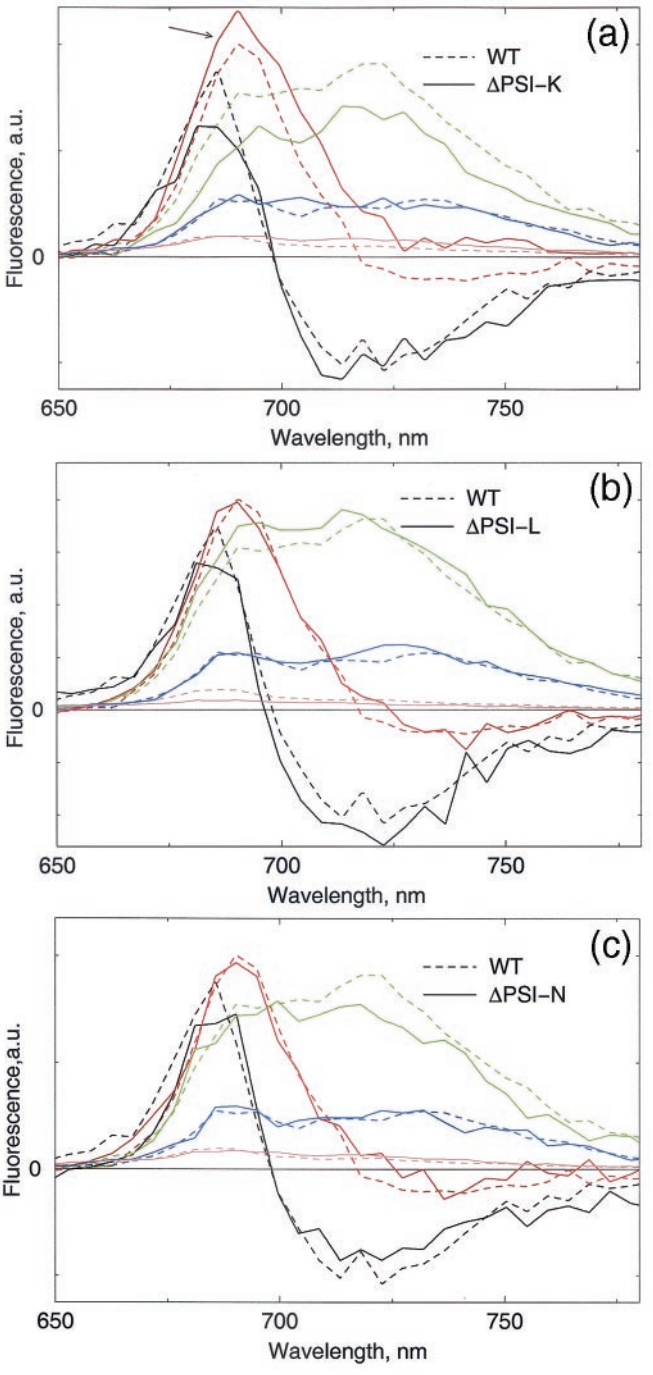

FIGURE 5 DAS of fluorescence decay after 475-nm excitation of isolated PSI-200 complexes from wild-type *Arabidopsis thaliana* (— — —) and its mutants (——) devoid of the PSI-K (*a*), PSI-L (*b*), or PSI-N (*c*) subunits. The black curves represent the 4.9-ps phases, the red curves the 16.5-ps phases, the green curves the 46-ps phases, and the blue curves the 114-ps phases. The 0.6-ps components were left out for simplicity. All spectra were scaled to the amplitudes of the wild-type spectra.

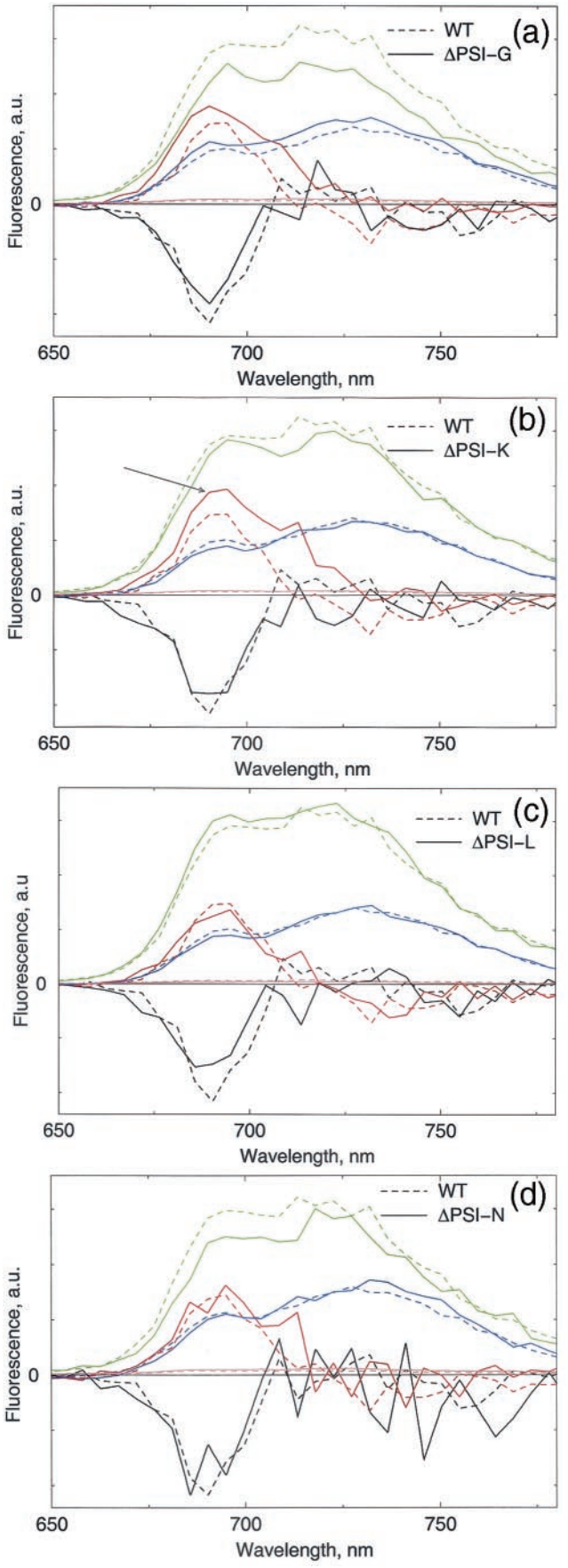

TABLE 3 Trapping proportion (percent) of each component upon 475-nm excitation after global analysis (the integrated area under each DAS of each mutant)

Component	Wild type	ΔPSI-K	ΔPSI-L	ΔPSI-N
16.5 ps	19	33	20	23
46 ps	56	41	58	51
114 ps	20	19	20	20
4.8 ns	5	7	3	6

The trapping in the 46- and 114-ps phases is entirely due to trapping by charge separation, whereas the 16.5-ps phase reflects a combination of trapping by charge separation and trapping in LHCI. The 4.8-ns phase reflects fluorescence decay of unconnected chlorophyll and LHCI complexes (see text).

the PSI-K mutant is slightly red-shifted compared with those of most other particles, in agreement with the idea that in this mutant, part of the more blue-absorbing LHCI antenna is missing (Jensen et al., 2000).

DISCUSSION

The results described in this paper provide new insight in the pigment-binding properties of the small PSI subunits PSI-G, PSI-K, PSI-L, and PSI-N of *Arabidopsis thaliana* and in their role in the excitation energy transfer and trapping processes in the PSI-200 complexes.

The plant lines devoid of PSI-L also had a 90% deficiency of PSI-H (Lunde et al., 2000), so the differences with the wild-type complexes actually reflect the absence of both proteins. The 5 K absorbance difference spectra with the PSI-200 complexes from the wild-type plants indicate that PSI-L and PSI-H of *Arabidopsis* bind Chl *a* and that these molecules absorb maximally at 688 and 667 nm. This result differs from that of the absence of PSI-L in *Synechocystis* sp. PCC 6803, which gave a main difference at 700 nm (Soukoulis et al., 1999). The role of PSI-L may, however, be different in green plants and cyanobacteria, because in the latter organisms it mediates trimerization (Chitnis and Chitnis, 1993), a process that probably requires the binding of calcium ions to PSI-L (Schwabe et al., 2001). Trimerization probably does not occur in green plants, but in these organisms the PSI-L subunit is closely associated with PSI-H, which does not occur in cyanobacteria and which is involved in the so-called state transitions (Lunde et al., 2000; Haldrup et al., 2001). If PSI-H indeed binds LHCII in state 2 (Haldrup et al., 2001), then the chlorophylls of PSI-H and PSI-L could very well be involved in the connection of the

FIGURE 6 DAS of fluorescence decay after 710-nm excitation of isolated PSI-200 complexes from wild-type *Arabidopsis thaliana* (— — —) and its mutants (——) devoid of the PSI-G (*a*), PSI-K (*b*), PSI-L (*c*), or PSI-N (*d*) subunits. The black curves represent the 4.8-ps phases, the red curves the 12-ps phases, the green curves the 47-ps phases, and the blue curves the 123-ps phases. All spectra were scaled to the amplitudes of the wild-type spectra.

TABLE 4 Trapping proportion (percent) of each component upon 710-nm excitation after global analysis (the integrated area under each DAS of each mutant)

Component	Wild type	ΔPSI-G	ΔPSI-K	ΔPSI-L	ΔPSI-N
12 ps	4	15	16	6	9
47 ps	66	51	58	67	57
123 ps	28	31	25	26	30
8.7 ns	2	3	2	1	3

The trapping in the 47- and 123-ps phases is entirely due to trapping by charge separation, whereas the 12-ps phase reflects a combination of trapping by charge separation and trapping in LHCI. The 8.7-ns phase reflects fluorescence decay of unconnected chlorophyll and LHCI complexes (see text).

antenna systems of the PSI core complex and LHCII. The relatively long wavelength of at least some of these chlorophylls would then be advantageous for the directed energy flow from LHCII to PSI.

It also appeared that the fluorescence spectra from the complexes without PSI-L and PSI-H gave relatively small contributions from unconnected chlorophylls, which can be explained by a relatively remote location of the chlorophylls of PSI-L (Jordan et al., 2001) and PSI-H. The excitation energy transfer and trapping dynamics, however, are indistinguishable from those of the wild type, which can be explained by the idea that a large part of the dynamics occurs in the peripheral antenna regions of the complex, which are far away from the location of the PSI-L and PSI-H proteins (Boekema et al., 2001).

The results on the PSI-200 complexes without PSI-N suggest that not just any change in the PSI protein composition causes a change in pigment organization. We did not find any indications for the binding of pigments by PSI-N,

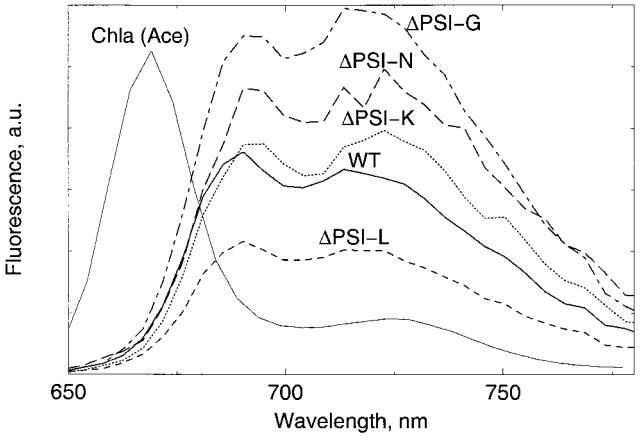

FIGURE 7 DAS of the long-lived components (8.7 ns) after 710-nm excitation of isolated PSI-200 complexes from wild-type *Arabidopsis thaliana* and its mutants devoid of the PSI-G, PSI-K, PSI-L, or PSI-N subunits, normalized as in Fig. 6. The thin solid line shows the fluorescence spectrum of Chl *a* in acetone with a lifetime of 6.2 ns after 400-nm excitation.

or for a role of PSI-N in the excitation energy transfer and trapping dynamics of the photosystem. PSI-N is a small extrinsic subunit at the lumen side and is very likely involved in the docking of plastocyanin (Haldrup et al., 1999).

PSI-G and PSI-K, on the other hand, are intrinsic membrane proteins, and for both proteins there are indications that they are involved in the binding of the peripheral LHCI antenna to the PSI core complex. In cyanobacteria, PSI-K is located far away from the symmetry axis of the complex and binds two chlorophyll molecules (Jordan et al., 2001). The binding of chlorophyll by PSI-K could not, however, be confirmed by our measurements, because the differences between the wild-type PSI-200 complexes and those without PSI-K are dominated by the partial absence of the Lhca2 and Lhca3 LHCI antenna proteins, in agreement with earlier results (Jensen et al., 2000). The trapping efficiencies in the three different kinetic phases (Tables 3 and 4) are in agreement with the partial absence of Lhca2 and Lhca3, because of the relatively prominent ~15-ps trapping phase (attributed to trapping from the core antenna chlorophylls) and the relatively weak ~50-ps trapping phase (attributed to trapping from the Lhca2 and Lhca3 chlorophylls). These results confirm the notion that the PSI-K protein belongs to the group of proteins that connect peripheral antenna and core complexes. The recently discovered PsbZ protein of photosystem II (Swiatek et al., 2001) also belongs to this group.

The PSI-G protein does not occur in PSI from cyanobacteria, and its absence does not give rise to a smaller LHCI content of the PSI-200 particles, although its absence may result in a weaker interaction between the PSI core and the LHCI antenna (Jensen et al., 2002). Our pigment analysis and low-temperature absorbance difference measurements indicate that PSI-G binds approximately two β-carotene molecules with a (5 K) absorption maximum of ~506 nm, which is more to the red than that of most other β-carotene molecules of the PSI core complex. We did not find evidence for chlorophyll binding to PSI-G, although the binding of a single chlorophyll can probably not be excluded. The absence of PSI-G resulted in an increased trapping efficiency within the ~15-ps phase at the expense of the ~50-ps phase. These results can possibly be explained by a partial detachment of peripheral antenna complexes from the PSI core during the measurements. Indeed, the mutant without the PSI-G protein showed the largest amount of badly connected LHCI (Fig. 7), in agreement with the weaker interaction between LHCI and the PSI core complex under mildly denaturing conditions (Jensen et al., 2002). The overall light-harvesting efficiency, however, is very similar in PSI-200 complexes with and without the PSI-G protein, which suggests that the strongly increased $NADP^+$ photoreduction rate without PSI-G (Jensen et al., 2002) is caused by an effect of PSI-G on the electron transfer properties of PSI. It remains to be clarified, however, in which way the PSI-G protein affects the electron transport rates of

PSI and whether any β-carotene molecules of PSI-G are essentially involved in this process.

This research was supported by the Netherlands Organization for Scientific Research via the Foundation of Earth and Life Sciences and by the Danish National Research Foundation. The visit of J.A.I. to Amsterdam was supported by the European Science Foundation by means of the ULTRA program.

REFERENCES

Beddard, G. S. 1998. Excitations and excitons in photosystem I. *Phil. Trans. R. Soc. Lond. A* 356:421–448.

Bibby, T. S., J. Nield, and J. Barber. 2001. Iron deficiency induces the formation of an antenna ring around trimeric photosystem I in cyanobacteria. *Nature.* 412:743–745.

Boekema, E. J., A. Hifney, A. E. Yakushevska, M. Piotrowski, W. Keegstra, S. Berry, K.-P. Michel, E. K. Pistorius, and J. Kruip. 2001b. A giant chlorophyll-protein complex induced by iron deficiency in cyanobacteria. *Nature.* 412:745–748.

Boekema, E. J., P. E. Jensen, E. Schlodder, J. F. L. van Breemen, H. van Roon, H. V. Scheller, and J. P. Dekker. 2001a. Green plant photosystem I binds light-harvesting complex I on one side of the complex. *Biochemistry.* 40:1029–1036.

Chitnis, P. R. 2001. Photosystem I: function and physiology. *Annu. Rev. Plant Physiol. Plant Mol. Biol.* 52:593–626.

Chitnis, V. P., and P. R. Chitnis. 1993. PsaL subunit is required for the formation of photosystem I trimers in the cyanobacterium *Synechocystis* sp. *PCC* 6803. *FEBS Lett.* 336:330–334.

Croce, R., D. Dorra, A. R. Holzwarth, and R. C. Jennings. 2000. Fluorescence decay and spectral evolution in intact photosystem I of higher plants. *Biochemistry.* 39:6341–6348.

Croce, R., G. Zucchelli, F. M. Garlaschi, R. Bassi, and R. C. Jennings. 1996. Excited state equilibration in the photosystem I light-harvesting I complex: P700 is almost isoenergetic with its antenna. *Biochemistry.* 35:8572–8579.

Croce, R., G. Zucchelli, F. M. Garlaschi, and R. C. Jennings. 1998. A thermal broadening study of the antenna chlorophylls in PSI-200, LHCI, and PSI core. *Biochemistry.* 37:17355–17360.

Du, M., X. Xie, Y. Jia, L. Mets, and G. R. Fleming. 1993. Direct observation of ultrafast energy transfer in PSI core antenna. *Chem. Phys. Lett.* 535–542.

Fromme, P., P. Jordan, and N. Krauss. 2001. Structure of photosystem I. *Biochim. Biophys. Acta.* 1507:5–31.

Ganeteg, U., Å. Strand, P. Gustafsson, and S. Jansson. 2001. The properties of the chlorophyll *a*/*b*-binding proteins Lhca2 and Lhca3 studied in vivo using antisense inhibition. *Plant Physiol.* 127:150–158.

Gibasiewicz, K., V. M. Ramesh, A. N. Melkozernov, S. Lin, N. W. Woodbury, R. E. Blankenship, and A. N. Webber. 2001. Excitation dynamics in the core antenna of PS I from *Chlamydomonas reinhardtii* CC 2696 at room temperature. *J. Phys. Chem. B.* 105:11498–11506.

Gobets, B., J. T. M. Kennis, J. A. Ihalainen, M. Brazzoli, R. Croce, I. H. M. van Stokkum, R. Bassi, J. P. Dekker, H. van Amerongen, G. R. Fleming, and R. van Grondelle. 2001a. Excitation energy transfer in dimeric light-harvesting complex I: a combined streak-camera/fluorescence upconversion study. *J. Phys. Chem. B.* 105:10132–10139.

Gobets, B., and R. van Grondelle. 2001. Energy transfer and trapping in photosystem I. *Biochim. Biophys. Acta.* 1507:80–99.

Gobets, B., I. H. M. van Stokkum, M. Rögner, J. Kruip, E. Schlodder, N. V. Karapetyan, J. P. Dekker, and R. van Grondelle. 2001b. Time-resolved fluorescence emission measurements of photosystem I particles of various cyanobacteria: A unified compartmental model. *Biophys. J.* 81: 407–424.

Haldrup, A., P. E. Jensen, C. Lunde, and H. V. Scheller. 2001. Balance of power: a view of the mechanism of photosynthetic state transitions. *Trends Plant Sci.* 6:301–305.

Haldrup, A., J. Naver, and H. V. Scheller. 1999. The interaction between plastocyanin and photosystem I is inefficient in transgenic *Arabidopsis* plants lacking the PSI-N subunit of photosystem I. *Plant J.* 17:689–698.

Haldrup, A., D. J. Simpson, and H. V. Scheller. 2000. Down-regulation of the PSI-F subunit of photosystem I (PSI) in *Arabidopsis thaliana*: the PSI-F subunit is essential for photoautotrophic growth and contributes to antenna function. *J. Biol. Chem.* 275:31211–31218.

Holzwarth, A. R. 1996. Data analysis of time-resolved measurements. *In* Biophysical Techniques in Photosynthesis. J. Amesz and A. J. Hoff, editors. Kluwer Academic Publishers, Amsterdam.75–92.

Ihalainen, J. A., B. Gobets, K. Sznee, M. Brazzoli, R. Croce, R. Bassi, R. van Grondelle, J. E. I. Korppi-Tommola, and J. P. Dekker. 2000. Evidence for two spectroscopically different dimers of light-harvesting complex I from green plants. *Biochemistry.* 39:8625–8631.

Ihalainen, J. A., P. E. Jensen, A. Haldrup, I. H. M. van Stokkum, R. van Grondelle, H. V. Scheller, and J. P. Dekker. 2001. Spectroscopic characterization of isolated PSI-200 complexes from plants devoid of the PSI-G, PSI-K, PSI-L and PSI-N subunits. *In* PS2001 Proceedings: 12th International Congress on Photosynthesis. CSIRO Publishing, Melbourne, Australia. S6–013.

Jansson, S. 1994. The light-harvesting chlorophyll *a*/*b* binding proteins. *Biochim. Biophys. Acta.* 1184:1–19.

Jensen, P. E., M. Gilpin, J. Knoetzel, and H. V. Scheller. 2000. The PSI-K subunit of photosystem I is involved in the interaction between light-harvesting complex I and the photosystem I reaction center core. *J. Biol. Chem.* 275:24701–24708.

Jensen, P. E., L. Rosgaard, J. Knoetzel, and H. V. Scheller. 2002. Photosystem I activity is increased in the absence of the PSI-G subunit. *J. Biol. Chem.* 277:2798–2803.

Jordan, P., P. Fromme, H. T. Witt, O. Klukas, W. Saenger, and N. Krauss. 2001. Three-dimensional structure of cyanobacterial photosystem I at 2.5 angstrom resolution. *Nature.* 411:909–917.

Kennis, J. T. M., B. Gobets, I. H. M. van Stokkum, J. P. Dekker, R. van Grondelle, and G. R. Fleming. 2001. Light harvesting by chlorophylls and carotenoids in the photosystem I core complex of *Synechococcus elongatus*: a fluorescence upconversion study. *J. Phys Chem. B.* 105: 4485–4494.

Kjaerulff, S., B. Andersen, V. S. Nielsen, J. S. Møller, and J. Okkels. 1993. The PSI-K subunit of photosystem I from barley (*Hordeum vulgare* L.): evidence for a gene duplication of an ancestral PSI-G/K gene. *J. Biol. Chem.* 268:18912–18916.

Knoetzel, J., A. Mant, A. Haldrup, P. E. Jensen, and H. V. Scheller. 2002. PSI-O, a new 10-kDa subunit of eukaryotic photosystem I. *FEBS Lett.* 510:145–148.

Lunde, C., P. E. Jensen, A. Haldrup, J. Knoetzel, and H. V. Scheller. 2000. The PSI-H subunit of photosystem I is essential for state transitions in plant photosynthesis. *Nature.* 408:613–615.

Melkozernov, A. N., V. H. R. Schmid, G. W. Schmidt, and R. E. Blankenship. 1998. Energy redistribution in heterodimeric light-harvesting complex LHCI-730 of photosystem I. *J. Phys. Chem. B.* 102: 8183–8189.

Pålsson, L. O., C. Flemming, B. Gobets, R. van Grondelle, J. P. Dekker, and E. Schlodder. 1998. Energy transfer and charge separation in photosystem I: P700 oxidation upon selective excitation of the long-wavelength antenna chlorophylls of *Synechococcus elongatus*. *Biophys. J.* 74:2611–2622.

Scheller, H. V., P. E. Jensen, A. Haldrup, C. Lunde, and J. Knoetzel. 2001. Role of subunits in eukaryotic photosystem I. *Biochim. Biophys. Acta.* 1507:41–60.

Schwabe, T. M. E., E. J. Boekema, S. Berry, P. R. Chitnis, E. Pistorius, and J. Kruip. 2001. Dynamics of photosystem I: Ca^{2+}-based oligomerization and response to iron deficiency by induction of a new antenna built by IsiA. *In* PS2001 Proceedings: 12th International Congress on Photosynthesis. CSIRO Publishing, Melbourne, Australia. S6–003.

Soukoulis, V., S. Savikhin, W. Xu, P. R. Chitnis, and W. S. Struve. 1999. Electronic spectra of PS I mutants: the peripheral subunits do not bind red chlorophylls in *Synechocystis* sp. PCC 6803. *Biophys. J.* 76:2711–2715.

Swiatek, M., R. Kuras, A. Sokolenko, D. Higgs, J. Olive, G. Cinque, B. Müller, L. A. Eichacker, D. B. Stern, R. Bassi, R. G. Herrmann, and F. A. Wollman. 2001. The chloroplast gene ycf9 encodes a photosystem II (PSII) core subunit, PsbZ, that participates in PSII supramolecular architecture. *Plant Cell.* 13:1347–1367.

Turconi, S., N. Weber, G. Schweitzer, H. Strotmann, and A. R. Holzwarth. 1994. Energy transfer and charge separation kinetics in photosystem I. II. Picosecond fluorescence study of various PS I particles and light-harvesting complex isolated from higher plants. *Biochim. Biophys. Acta.* 1187:324–334.

van Grondelle, R., J. P. Dekker, T. Gillbro, and V. Sundström. 1994. Energy transfer and trapping in photosynthesis. *Biochim. Biophys. Acta.* 1187:1–65.